Journal of Groundwater Science and Engineering
ISSN 2305-7068
Indexed by ESCI CABI CSA
Scopus GeoRef AJ CNKI

Experimental and numerical investigation for energy dissipation of supercritical flow in sudden contractions

Rasoul Daneshfaraz, Ehsan Aminvash, Reza Esmaeli, Sina Sadeghfam, John Abraham

Citation:
Rasoul Daneshfaraz, Ehsan Aminvash, Reza Esmaeli, Sina Sadeghfam, John Abraham. Experimental and numerical investigation for energy dissipation of supercritical flow in sudden contractions[J]. *Journal of Groundwater Science and Engineering*, 2020, 8(4): 396-406.

View online: https://doi.org/10.19637/j.cnki.2305-7068.2020.04.009

DOI: 10.19637/j.cnki.2305–7068.2020.04.009

Experimental and numerical investigation for energy dissipation of supercritical flow in sudden contractions

Rasoul Daneshfaraz[1*], Ehsan Aminvash[2], Reza Esmaeli[2], Sina Sadeghfam[1], John Abraham[3]

[1] Department of Civil Engineering, Faculty of Engineering, University of Maragheh, Maragheh, Iran.
[2] Department of Civil Engineering, University of Maragheh, Maragheh, Iran.
[3] University of St Thomas, School of Engineering, St Paul, USA.

Abstract: Dealing with kinetic energy is one of the most important problems in hydraulic structures, and this energy can damage downstream structures. This study aims to study energy dissipation of supercritical water flow passing through a sudden contraction. The experiments were conducted on a sudden contraction with 15 cm width. A 30 cm wide flume was installed. The relative contraction ranged from 8.9 to 9.7, where relative contraction refers to the ratio of contraction width to initial flow depth. The Froude value in the investigation varied from 2 to 7. The contraction width of numerical simulation was 5~15 cm, the relative contraction was 8.9~12.42, and the Froude value ranged from 8.9~12.42. In order to simulate turbulence, the k-ε RNG model was harnessed. The experimental and numerical results demonstrate that the energy dissipation increases with the increase of Froude value. Also, with the sudden contraction, the rate of relative depreciation of energy is increased due to the increase in backwater profile and downstream flow depth. The experimentation verifies the numerical results with a correlation coefficient of 0.99 and the root mean square error is 0.02.

Keywords: Relative energy dissipation; Hydraulic jump; Sudden contraction

Received: 25 Feb 2020/ Accepted: 22 May 2020

Introduction

As one of the critical issues for many hydraulic structures, kinetic energy of water flow must be dissipated by water-control structures. If the flow energy is not reduced, downstream structures may be damaged or destroyed. Energy dissipation is proportional to the flow turbulence and the contraction of flow can significantly decrease the energy. A sudden contraction in the flow passage will lead to a hydraulic jump, which dissipates the destructive energy. Experiments and theoretical studies show that stilling basins, bed roughness, and screens have energy dissipation effects.

Yasuda and Hager (1995) studied hydraulic jumps in a rectangular channel with a gradual contraction in supercritical flow for relative contractions of 0.3~0.8 and with lengths of 1 080 mm, 1 550 mm and 2 080 mm. The results show that with the increase of upstream Froude number, the depth of downstream flow and the end of the contraction zone increase. WU Bao-sheng and Molinas (2001) studied the subcritical flow behavior using a short contraction. Their results show that the discharge coefficient is mainly affected by the relative contraction. Dey and Raikar (2007) studied the characteristics of subcritical flow in scouring pits induced by a long contraction. The results indicate that the scour depth increases with the decrease of relative shrinkage and the increase of wall roughness.

Jan and Chang (2009) studied hydraulic jumps

*Corresponding author. E-mail: daneshfaraz@yahoo.com

in the contraction of an inclined rectangular chute. In the contraction zone, the flume width decreased linearly at different angles and numbers. The results show that as the Froude value increases, the energy dissipation increases. Also, the relative hydraulic jump length decreases with the decrease of river bed inclination. Although the study of sudden contraction energy dissipation in supercritical flow is limited, this brief literature focuses on the study of hydraulic jumps and energy dissipation in those circumstances.

Rajaratnam and Hurtig (2000) examined energy dissipation of supercritical flow through screens with a porosity of 40%. The results show that as the Froude value increases, energy dissipation also increases. Studies on the effect of the thickness and percentage of porosity of screens on energy dissipation by Çakir (2003) were also considered. The results show that screens are effective in energy dissipation and the thickness of screens does not have much effect. Bozkus *et al*. (2007) researched the effect of screens on energy dissipation. It is shown that 40% porosity and multiple arranged screens can dissipate more energy than a traditional hydraulic jump. Sadeghfam *et al*. (2015) employed screens with porosity of 40% and 50% and for Froude values between 2.5 and 8.5. Their research shows that the energy dissipation effect of screens is better than that of free and submerged hydraulic jumps. They also showed that double screens performed better than the single screen. Nayebzadeh *et al*. (2020) examined the numerical characteristics of flow in vertical drops with a gradual expanding wall. The results show that the simultaneous use of divergence and screens increases the dissipation. Investigations just like the characteristics of a hydraulic jump and its type in diverging stilling basins with smooth beds have also been performed by researchers such as Rajaratnam and Subramanya (1968), Herbrand (1973), Bremen and Hager (1993), Alhamid (2004) and Matin *et al*. (2008).

In recent years, different numerical methods and softwares have been used to simulate the destructive kinetic energy dissipation on structures. Sharif and Rostami (2014) used the Flow-3D software to analyze the effect of flow separation on energy dissipation in a compound bucket. They simulated three buckets with angles of 20, 40 and 80 degrees. Their researches show that a bucket with an angle of 20 degrees is the most efficient and consumes more energy than other buckets. Jamil and Khan (2010) studied energy dissipation and hydraulic characteristics of a hydraulic jump in a circular channel section. The results show that with the increase of Froude number, the relative length of the hydraulic jump and total energy dissipation increase. Daneshfaraz *et al*. (2014a, 2014b) examined the numerical flow on the stepped spillway using Fluent. The results show a significant increase in the energy dissipation on the stepped spillway. Also, by examining the flow on the ogee, stepping spillways numerically, comparing the finite element methods and the limited volume, they concluded that the finite volume method has much more acceptable results than the finite element method. Lebdiri *et al*. (2018) compared the finite element method with the finite volume method for free surface profile flows. The results show that both methods can estimate the free surface profile well. Ghazi *et al*. (2019) numerically investigated the hydraulic characteristics and cavitation in the spillway of Shahid using the finite volume method. They observed that the results of the finite volume method were close to the measured data and there was no cavitation in the spillway. The study of hydraulic jump in different conditions of the channel bed using VOF and CFD methods has also been done by other researchers such as Chippada *et al*. (1994), Babaali *et al*. (2014), Castillo *et al*. (2014). Numerical and laboratory studies of energy dissipation caused by a hydraulic jump on ogee and stepped spillways have been performed by researchers such as Ghaderi and Abbasi (2019), Daneshfaraz *et al*. (2019a, 2019b, 2019c), Zhou *et al*. (2020), Ghaderi *et al*. (2020) and Daneshfaraz *et al*. (2017).

To study the energy dissipation of water flow, previous studies have focused on different dissipation structures, such as gradual contractions and contracting chutes. To the present authors' best knowledge, there are limited studies on energy dissipation of supercritical flow through a sudden contraction with different relative contractions.

1 Materials and methods

1.1 Experimental set-up

In this study, a horizontal open channel flume 0.3 m in width, 0.5 m in depth and with a 5 m length was adopted. The experimental facility is located at the University of Maragheh in Iran. The walls are made from Plexiglass in order to provide good visibility. The inlet flow and flow depths were measured by two rotameters with an absolute error of 2%. They were installed at the outlet of the pump and measured with a point gage with an accuracy of 1 mm. Supercritical flow conditions were generated using a sluice gate with a 1 cm thickness and a 2.60 cm opening with the distance of 1.5 m away from the inlet of flow. In terms of building a sudden contraction in the flow path, panels were installed 1.5 m from the sluice gate. Two triangular panels of 22.5 cm length were used at the end of the structure to reduce the turbulence. Fig. 1 provides a detailed schematic representation of the experimental flume, indicating measurement locations. Table 1 presents the discharge and the Froude values used in the experiments.

Table 1 Discharge and Froude number used in the experiments

Num	10	9	8	7	6	5	4	3	2	1
Q (L/m)	750	700	650	600	550	500	450	400	350	300
Fr value	6.36	5.97	5.67	5.28	4.90	4.52	4.13	3.74	3.36	2.97

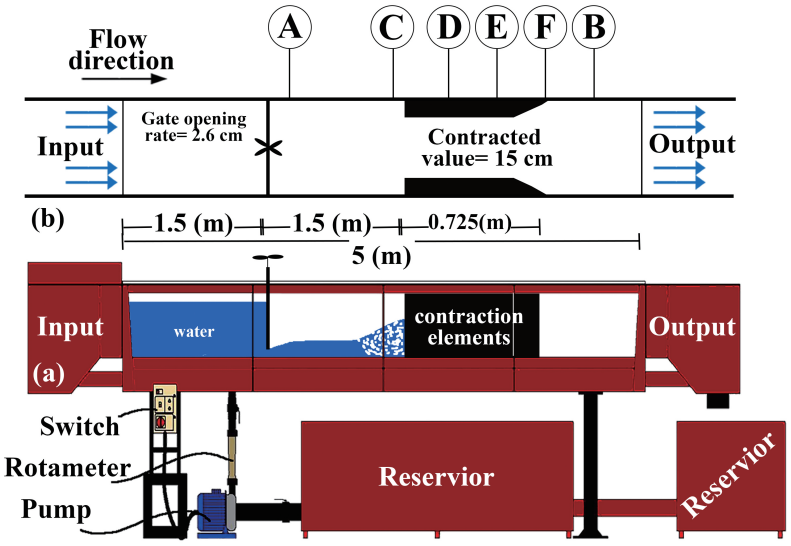

Fig. 1 (a) Schematic figure of the flume; (b) details in the plan view

1.2 Flow-3D and the simulation features

As a powerful computational fluid dynamic modeling software, Flow-3D can help engineers better understand many flow processes. In Flow-3D, free surfaces are modeled with the volume of fluid (VOF) technique, which has all the recommended components for successful treatment of the free surface. Flow-3D solves the continuity and momentum equations, including the turbulence models such as the k-ε model, the k-ε model and large eddy simulation. The general forms of the continuity and momentum equations are presented in Equation 1 and Equation 2, respectively, as follows (Ghaderi *et al*. 2020):

$$\frac{\partial Ui}{\partial \chi j}=0 \quad (1)$$

$$\frac{\delta Ui}{\delta ti}+\rho Ui\frac{\partial Ui}{\partial \chi i}+\frac{\partial P}{\partial \chi i}+\frac{\partial}{\partial \chi i}(\mu\frac{\partial Ui}{\partial \chi j}-pu'ju'j)+\rho gi \quad (2)$$

Where: U_i, u'_i are average and fluctuating velocities in the x_i direction respectively, x_i= (x, y, z), U_i= (U, V, W) and u'_i= (u', v', w'). The symbols ρ, μ, P and g_i are density, dynamic viscosity, pressure, and gravitational acceleration respectively. Instantaneous velocity is defined as u_i= U_i+u'_i for the three directions.

Table 2 shows comparison of the results with k-ε (RNG), and k-ω turbulence models in terms of R^2 and NRMSE coefficients.

Table 2 Comparing experimental with numerical Froude value in turbulence models

	Methods		
	RNG	k-ε	k-ω
R^2	0.995	0.956	0.937
NRMSE	0.02	0.09	0.11

According to Table 2, the RNG turbulence model shows the best results, so it is selected as the turbulence model for all simulations. Table 3 shows the range of variables measured during the experiment.

Table 3 Range of measured variables

Contraction (cm)	Discharge (L/s)	Upstream depth (cm)	Froude value	Downstream depth (cm)	Reynolds value
5	5.5~12.4	2.01~2.05	2.48~5.18	4.4~8.9	75 000~141 260
10	5.5~12.4	2.01~2.05	2.44~4.91	4.55~9.2	76 500~159 000
15	5.5~12.4	1.54~1.62	2.72~6.53	4.72~10.2	59 000~238 000

1.3 Computational grid and boundary conditions

Table 4 provides information about the computational mesh. In the Cartesian coordinate system, the mesh size of all models is 0.005 m which was determined using a mesh-refinement study.

Table 4 Details of the computational mesh

Size of cells	X direction	Mesh plane	Y direction	Mesh plane	Z direction	Mesh plane
0.005 (m)	1	2	1	2	1	2
	1.00	3.80	0.00	0.30	0.00	0.40

The boundary conditions are listed in Table 5. The flow domain comprises of seven components, including (1) the inflow boundary; (2) the sluice gate which generates supercritical flow; (3) the reservoir; (4) the sudden contraction; (5) the outflow boundary; (6) the bottom and side boundaries; and (7) the top boundary. Fig. 2 shows the flow domain, meshing features and boundary conditions for the 5 cm width contraction.

Table 5 Boundary conditions

X boundaries		Y boundaries		Z boundaries	
Min	Max	Min	Max	Min	Max
Volume Flow Rate (VFR)	Outflow	Wall	Wall	Wall	Symmetry

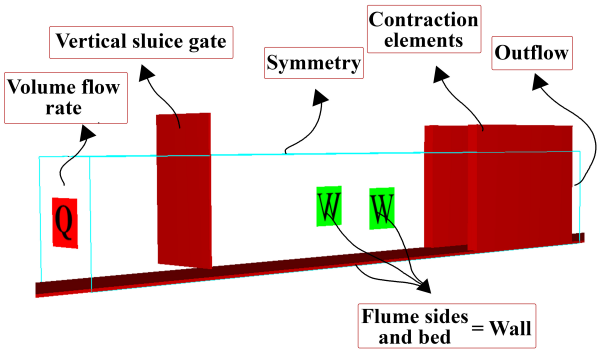

Fig. 2 Schematic of grid solution, boundary conditions and meshing details

The specific energy, depth, and the critical depth are used to calculate energy dissipation. Equation 3 and Equation 4 are used to calculate the upstream and downstream specific energy, respectively. Due to the existence of turbulence, the depth of water flow cannot be measured accurately after the hydraulic jump. Consequently, Equation 5 and Equation 6 are used to calculate the flow depth after the hydraulic jump and the critical depth, respectively. The classical hydraulic equations are presented in Table 6.

Table 6 Classical equations of energy and hydraulic jump

$$E_0 = y_0 + \frac{V_0^2}{2_g} = y_0 + \frac{q^2}{2gy_0^2} \quad (3)$$

$$E_1 = y_1 + \frac{V_1^2}{2g} = y_1 + \frac{q^2}{2gy_1^2} \quad (4)$$

$$y_1 = \frac{y_0}{2} = (-1 + \sqrt{1 + 8Fr_0^2}) \quad (5)$$

$$y_{cr} = \sqrt[3]{\frac{q^2}{g}} \quad (6)$$

$$F_{cr} = \frac{V_0}{\sqrt{gy_0}} \quad (7)$$

$$E_r = \frac{x_{Exp} - x_{Num}}{E_{Exp}} \times 100 \quad (8)$$

$$RMSE = \sqrt{\frac{1}{n}\sum\left[x_{Exp} - x_{Num}\right]^2} \quad (9)$$

$$NRMSE = \frac{RMSE}{x_{Max} - x_{Min}} \quad (10)$$

Where: E_0 and E_1 mean specific energy upstream and downstream; y_0 and y_1 refer to the upstream flow depth and the flow depth after the hydraulic jump; V_0 and V_1 are upstream and downstream velocities, respectively; q is the discharge per unit width; g is the gravity acceleration; F_{r0} is the Froude value of the upstream flow; and y_{cr} is the critical depth.

The relative error, RMSE, and NRMSE are calculated based on Equation 8, Equation 9 and Equation 10, respectively.

1.4 Dimensional analysis

Using dimensional analysis, the functional relationship of governing parameters is as follows:

$$s = \phi[Q, Fr_0, V, W, B, l, d, D, E_0, E_1, y_0, y_1, ycr, g, \rho, \mu L] \quad (11)$$

Where: S is the energy dissipation rate; Q is the flow discharge; F_{r0} is the upstream Froude number; V is the fluid velocity; W means the channel width; B is the contraction width; l refers to the length of the contraction; d equals to the sluice gate opening; y_0 is the flow depth before the jump; y_1 shows the flow depth after the jump; y_{cr} is the critical depth; g represents the gravity acceleration; ρ is the density; μ is the dynamic viscosity; L is the length of jump. Based on the Buckingham theorem with repeating variables p, g and y_0, the non-dimensional parameters are produced:

$$\phi\left[Fr_o, \mathrm{Re}_0, \frac{W}{y_0}, \frac{E_0}{y_0}, \frac{E_1}{y_0}, \frac{l}{y_0}\frac{B}{y_0}, \frac{d}{y_0}, \frac{y_{cr}}{y_0}, \frac{L}{y_0}\right] = 0 \quad (12)$$

Note that in the present study, the Reynolds number is neglected due to turbulence. The channel width, contraction length and gate opening are constant during the test, so their changes are ignored. As the relative jump length, relative critical depth and relative contraction are beyond the scope of this study, the independent dimensionless parameters are defined as follows:

$$\frac{\Delta E}{E_0} = \phi\left[Fr_0, \frac{E_0}{y_0}, \frac{E_1}{y_0}\right] \quad (13)$$

2 Results and discussion

2.1 Laboratory observations

After the laboratory model was constructed and the flow discharge valve was open ed, the upstream liquid accelerates near the gate to a critical speed, and then further accelerates to a supercritical state. When the flow reaches the entrance of contraction, there will be a reversed flow and hydraulic jump, and the depth of the contraction zone will increase. Therefore, when the water flows through the contraction, the turbulence intensity increases and bubble entrainment occurs. The measurements revealed that the flow velocity increases by increasing the discharge rate.

2.2 Experimental results

Fig. 3 shows the relative energy dissipation in the sudden contraction with 15 cm width. The figure shows that the sudden contraction leads

to the increase of the relative energy dissipation downstream and upstream.

According to Fig. 3a and Fig. 3b, the relative energy dissipation increases with the increase of Froude value. When the supercritical flow impacts the contraction elements, the turbulence intensity and bubble entrainment increase and the corresponding energy dissipation increases through the reverse flow and hydraulic jump.

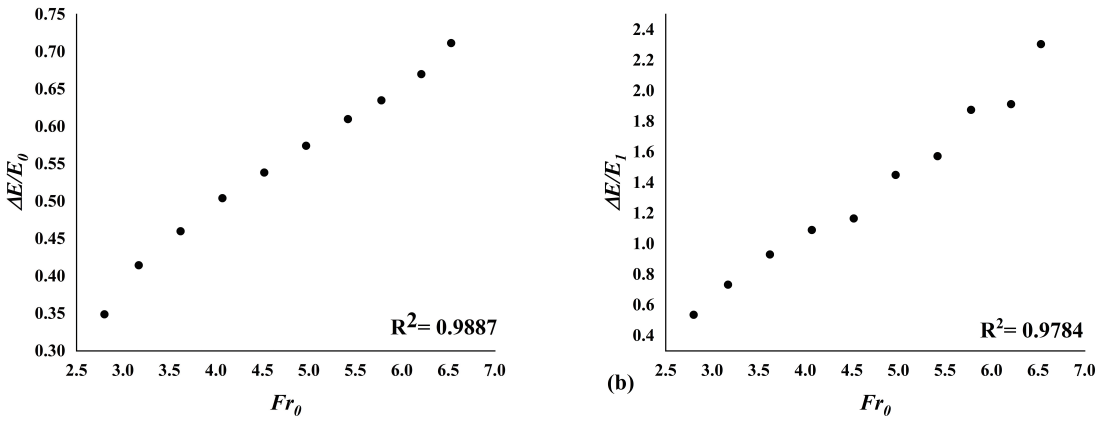

Fig. 3 Relative energy dissipation: (a) at upstream; (b) at downstream

2.3 Results of Flow-3D calculations

2.3.1 Validation

The Flow-3D results are verified by comparison with experimental data for 15 cm sudden contractions. The series of images in Fig. 4 compare the experimental and numerical results.

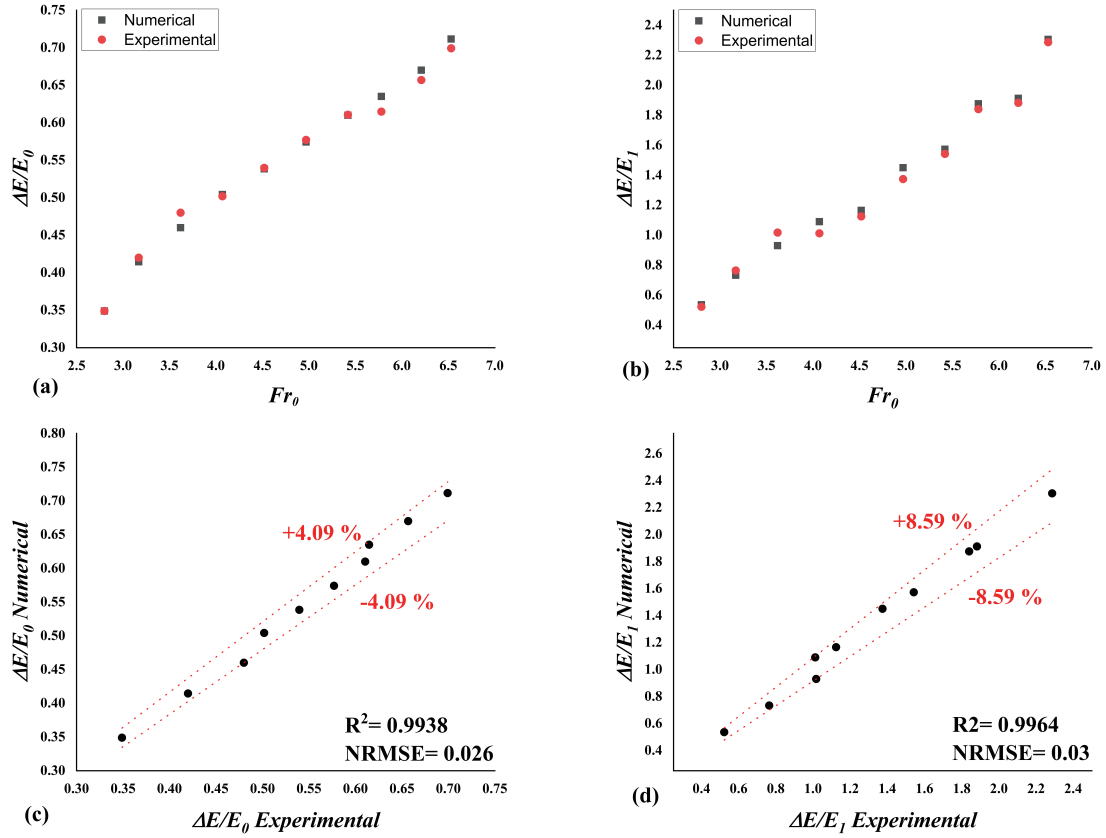

Fig. 4 Comparison between experimental and numerical results of: (a, b) Upstream and downstream relative energy dissipation; (c, d) Upstream and downstream energy dissipation

Fig. 4c and Fig. 4d show a comparison of the energy dissipation in the upstream and downstream flows, respectively. As shown by the R2 and NRMSE, the numerical results agree with the experimental results.

2.3.2 Relative energy dissipation

Turbulence occurs when the flow strikes the contraction element. The simulation time step is 0.009 seconds and the final time is 15 seconds, sufficient to obtain stable flow conditions. The simulation time stopped at 10 seconds when the steady conditions had been achieved. After the simulations, the required parameters for the energy dissipation were extracted and then the specific energy rate upstream and downstream were calculated based on Equation 3 and Equation 4. Finally, the relative energy was been calculated.

(1) Relative energy dissipation in the 5 cm contraction

The results were analyzed using the parameters of upstream relative energy dissipation ($\Delta E/E_0$) and downstream relative energy dissipation ($\Delta E/E_1$) based on the upstream flow Froude number and the relative contraction. Fig. 5 shows the relative energy dissipation variations with the upstream flow Froude value as well as the relative contraction.

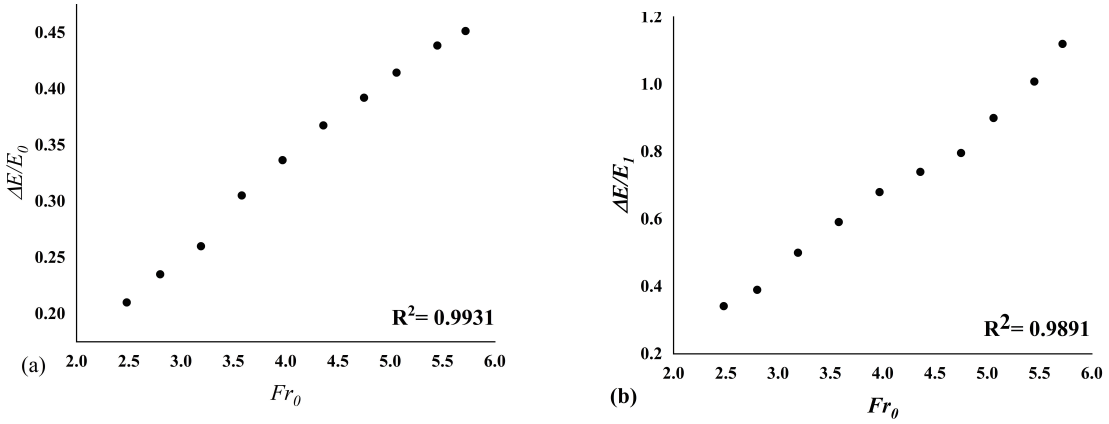

Fig. 5 Relative energy dissipation for a 5 cm contraction: (a) At upstream (b) at downstream

Fig. 5a and Fig. 5b indicate that the relative energy dissipation rate upstream and downstream of the contraction increases with the upstream Froude number. As the Froude number increases, the velocity increases and the flow contracts more rapidly. Reversed flow is a major reason for energy dissipation. In addition, the hydraulic jump, variation in flow regime, and increase of turbulence and air entrainment at the contraction zone are contributors.

By considering the results for a 5 cm width contraction, Equation 14 and Equation 15 were adopted to estimate the relative energy dissipation in the upstream and downstream regions, respectively.

$$\begin{aligned} &\frac{\Delta E}{E_0} = -0.00584 Fr_0^2 + 0.124 Fr_0 - 0.0678 \\ &R^2 = 0.999 \\ &NRMSE = 0.01 \end{aligned} \tag{14}$$

$$\begin{aligned} &\frac{\Delta E}{E_0} = -0.00189 Fr_0^2 + 0.0723 Fr_0 - 0.0608 \\ &R^2 = 0.990 \\ &NRNSE = 0.025 \end{aligned} \tag{15}$$

These equations estimate the numerical values of the relative energy dissipation with a maximum relative error of 3.95% and 9% for upstream and downstream, respectively. Fig. 6 compares the numerical and calculated values of the relative energy dissipation based on Equations 14 and Equation 15.

(2) Relative energy dissipation in the 10 cm contraction

Fig. 7 shows the change of relative energy dissipation in a 15 cm wide contraction and reveals that the use of sudden contraction in supercritical flow increases the upstream and downstream energy dissipation. Fig. 7a and Fig. 7b show the upstream and downstream relative energy dissipation, respectively, as a function of the upstream Froude value.

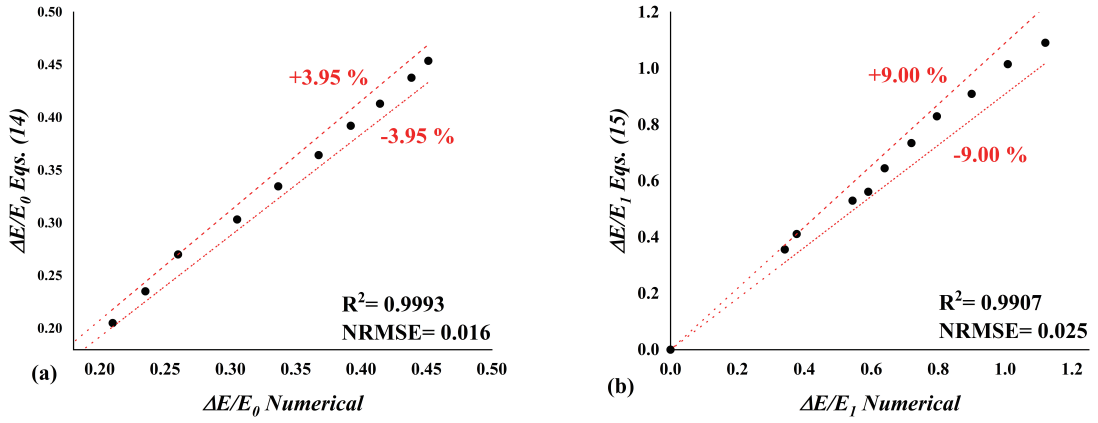

Fig. 6 Comparison between upstream/downstream relative energy dissipation and Equation 14 and Equation 15

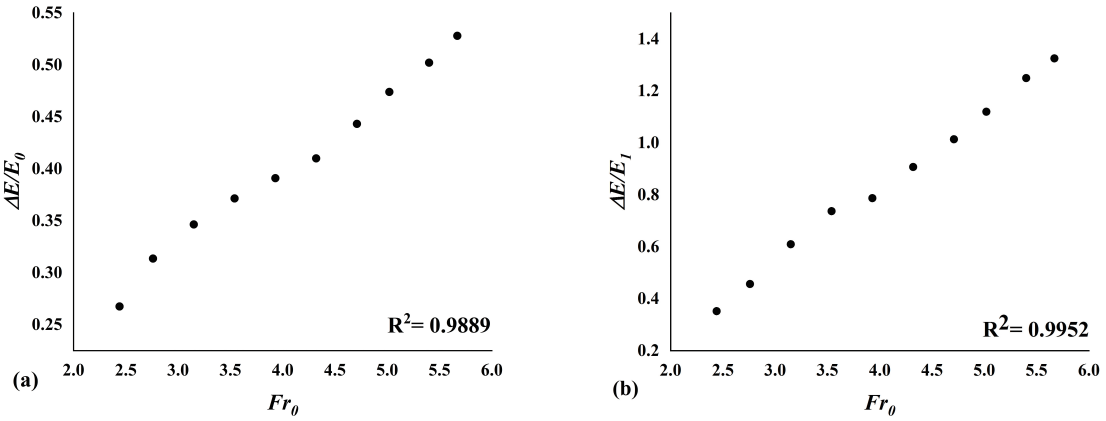

Fig. 7 Relative energy dissipation for a 10 cm contraction: (a, b) Upstream and downstream relative energy dissipation

These figures clearly show that the relative energy dissipation rate increases with the upstream Froude number. With the increase of discharge rate, the Froude value and flow velocity in the upstream increase. When the high-velocity flow hits the contraction elements, reversed flow and a hydraulic jump occur. In fact, the hydraulic jump can lead to air entrainment, energy dissipation and low-velocity flow.

Equation 16 and Equation 17 are used to estimate the relative energy dissipation upstream and downstream, respectively by considering the output data of 10 cm wide contraction simulation.

$$\frac{\Delta E}{E_0} = 7.02\times10^{-5} Fr_0^{\,2} + 0.0738 Fr_0 - 0.101$$
$$R^2 = 0.989 \qquad (16)$$
$$NRMSE = 0.021$$

$$\frac{\Delta E}{E_0} = -0.00068 Fr_0^{\,2} + 0.298 Fr_0 - 0.352$$
$$R^2 = 0.995 \qquad (17)$$
$$NRMSE = 0.022$$

These equations are used to estimate the numerical values of the relative energy dissipation with a maximum relative error of 5.33% and 5.79% for the upstream and downstream, respectively. Fig. 8 shows the comparison between the numerical and calculated values.

2.3.3 A comparison of energy dissipation in the models

Fig. 9 illustrates a comparison of the relative energy dissipation for different Froude values and for all three models. Also, Fig. 9a and Fig. 9b show the energy dissipation upstream and downstream of the contraction element, respectively.

As seen in Fig. 10, as the upstream Froude value increases, the energy dissipation in all the three models increases so that the energy dissipa-tion for 15 cm contraction is greater than that of 5 cm and 10 cm contractions. The result

shows that the Froude value increases with the discharge rate and velocity. The high-velocity flow hits the contraction elements and the hydraulic jump occurs, leading to the air entrainment and energy dissipation in the contraction zone. The reversed flow resulting from the collision of the high-velocity flow to the contraction increases. These phenomena intensify as the Froude number increases.

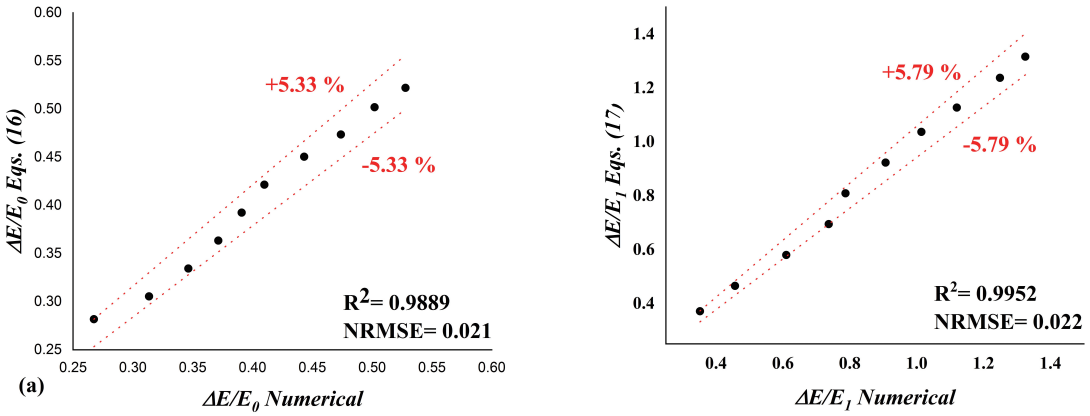

Fig. 8 Comparison between upstream and downstream relative energy dissipation with Equation 16 and Equation 17

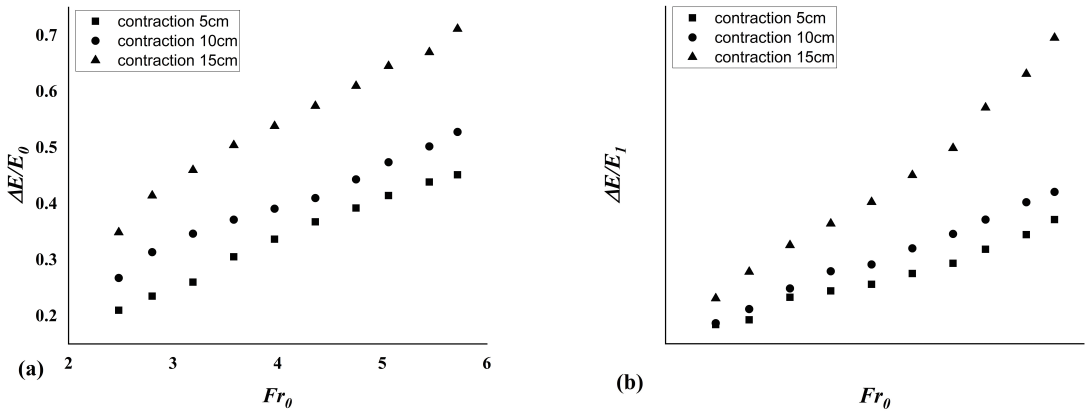

Fig. 9 Comparison of relative energy dissipation in models: (a) at upstream (b) at downstream

3 Conclusions

This study aimed to investigate the energy dissipation of supercritical fluid under sudden contraction by numerical and experimental methods. In the present study, the VOF method was used to simulate free surface flow and the RNG method was selected for the turbulence model. The results showed that the Froude value upstream of the sudden contraction calculated by the numerical method has a positive correlation with the experimental data. The efficiency of a short contraction with a supercritical flow has a significant effect on the dissipation of destructive kinetic energy. Also, increasing the width of the sudden contraction increases the downstream flow depth and the relative energy dissipation. In this study, three contraction sizes of 5 cm, 10 cm and 15 cm were used. In these three models, by increasing the Froude value of upstream, the relative energy dissipation of 15 cm contraction is more than 10 cm.

References

Alhamid AA. 2004. S-jump characteristics on sloping basins. Journal of Hydraulic Research, 42(6): 657-662.

Babaali H, Shamsai A, Vosoughifar H. 2015. Computational modeling of the hydraulic

jump in the stilling basin with convergence walls using CFD codes. Arabian Journal for Science and Engineering, 40: 381-395.

Bozkus Z, Pinar C, Metin G. 2007. Energy dissipation by vertically placed screens. Canadian Journal of Civil Engineering, 34(4): 557-564.

Bremen R, Hager WH. 1993. T-jump in abruptly expanding channel. Journal of Hydraulic Research, 31(1): 61-78.

Çakir P. 2003. Experimental investigation of energy dissipation through screens. Ph.D thesis. Ankara: Middle East Technical University.

Chippada S, Ramaswamy B, Wheeler MF. 1994. Numerical simulation of hydraulic jump. International Journal for Numerical Methods in Engineering, 37: 1381-1397.

Castillo LG, Carrillo JM, Carcía JT. 2014. Numerical simulations and laboratory measurements in hydraulic jumps. 11th International conference on hydroinformatics.

Daneshfaraz R, Sadeghfam S, Kashani M. 2014a. Numerical simulation of flow over stepped spillways. Research in Civil and Environmental Engineering. 2(04): 190-198.

Daneshfaraz R, Birol K, Sadeghfam S, *et al*. 2014b. Simulation of flow over ogee and stepped spillways and comparison of finite element volume and finite element methods. Journal of Water Resource and Hydraulic Engineering, 3(2): 37-47.

Daneshfaraz R, Minaei O, Abraham JP, *et al*. 2019a. 3-D Numerical simulation of water flow over a broad-crested weir with openings. ISH Journal of Hydraulic Engineering, 1-9.

Daneshfaraz R, Mirzaee R, Ghaderi A, *et al*. 2019b. The S-jump's characteristics in the rough sudden expanding stilling basin, AUT Journal of Civil Engineering. doi: 10.22060/ajce.2019.16427.5586.

Daneshfaraz R, Dasineh M, Ghaderi A, *et al*. 2019c. Numerical modeling of hydraulic properties of sloped broad crested weir. AUT Journal of Civil Engineering. doi: 10.22060/ajce.2019.16184.5574.

Daneshfaraz R, Ghaderi A. 2017. Numerical investigation of inverse curvature ogee spillways. Civil Engineering Journal, 3(11): 1146-1156.

Dey S, Raikar RV. 2007. Characteristics of horseshoe vortex in developing scour holes at piers. Journal of Hydraulic Engineering, 133(4): 399-413.

Ghaderi A, Abbasi S, Abraham J, *et al*. 2020. Efficiency of trapezoidal labyrinth shaped stepped spillways. Flow Measurement and Instrumentation. https://doi.org/j.flowmeasinst.2020.101711

Ghaderi A, Abbasi S. 2019. CFD simulation of local scouring around airfoil-shaped bridge piers with and without collar. Sadhana, 44(10): 216.

Ghazi B, Daneshfaraz R, Jeihouni E. 2019. Numerical investigation of hydraulic characteristics and prediction of cavitation number in Shahid Madani Dam's Spillway. Journal of Groundwater Science and Engineering, 7(4): 323-332.

Herbrand K. 1973. The spatial hydraulic jump. Journal of Hydraulic Research, 11(3): 205-218.

Jamil M, Suhail AK. 2010. Theoretical study of hydraulic jump in circular channel section. ISH Journal of Hydraulic Engineering, 16(1): 1-10.

Jan C, Chang C. 2009. Hydraulic jumps in an inclined rectangular chute contraction. Journal of Hydraulic Engineering, 135(11): 949-958.

Lebdiri F, Seghir A, Berreksi A. 2018. Finite element and finite volume method for simulation of free surface flows: Application to spillways. 2nd National Conference on Computational Fluid Dynamics and Technology at SSRN 3373179.

Matin MA, Hasan MR, Islam MA. 2008. Experiment on hydraulic jump in sudden expansion in a sloping rectangular channel. Journal of Civil Engineering (IEB), 36(2): 65-77.

Nayebzadeh B, Lotfollahi yaghin MA, Daneshfaraz R. 2020. Numerical investigation of hydraulic characteristics of vertical drops with screens and gradually wall expanding. Amirkabir Journal of Civil Engineering (In Persian).

Rajaratnam N, Hurtig KI. 2000. Screen-type energy dissipator for hydraulic structures. Journal of Hydraulic Engineering, 126(4): 310-312.

Rajaratnam N, Subramanya K. 1968. Hydraulic jumps below abrupt symmetrical expansions. Journal of the Hydraulics Division, 94(2): 481-504.

Sadeghfam S, Akhtari AA, Daneshfaraz R, *et al*. 2015. Experimental investigation of screens as energy dissipaters in submerged hydraulic jump. Turkish Journal of Engineering and Environmental Sciences, 38(2): 126-138.

Sharif N, Rostami A. 2014. Experimental and numerical study of the effect of flow sepration on dissipating energy in compound bucket. APCBEE Procedia, 9: 334-338.

WU Bao-sheng, Molinas A. 2001. Choked flows through short contractions. Journal of Hydraulic Engineering, 127(8): 657-662.

Yasuda Y, Hager W. 1995. Hydraulic jump in channel contraction. Canadian Journal of Civil Engineering, 22(5): 925-933.

Zhou Y, Wu J, Ma F, *et al*. 2020. Uniform flow and energy dissipation of hydraulic jump stepped spillways. Water Supply. https://doi.org/10.2166/ws.2020.056